MODELLING THE ENERGY PRODUCTION IN STELLAR CORES

Carlsen, J.*

(Dated: March 12, 2023)

The two processes for converting hydrogen into helium are the main producers of energy in hydrogen-burning stars. Being able to take advantage of modern technology in order to produce accurate models of stellar energy production, can contribute to expanding the horizon of human knowledge into the universe that surrounds us. The content of this paper includes estimations for the temperature dominance regions for the different PP branches and the CNO cycle, the latter being consistent with that of Iliadis (2015), i.e. for $T > 10^8$ K. For temperatures below $7.0 \cdot 10^4$ K, we find that the PP1 branch is dominant. PP2 takes over between $7.0 \cdot 10^4$ K and $2.5 \cdot 10^7$ K before the PP3 branch dominates for temperatures up to $1.2 \cdot 10^8$ K.

I. INTRODUCTION

After Francis W. Aston discovered that the mass of a helium atom is slightly less than four hydrogen atoms in 1920, Sir Arthur Eddington suggested that the discovery explained the energy generation in the Sun (Iliadis 2015), more precisely via the conversion of hydrogen to helium. It was believed that the temperature in the Sun was too low to overcome the Coulomb barrier and initiate fusion reactions. Following George Gamow's calculation of the quantum mechanical probability for particles to tunnel through potential barriers in 1928, the first nuclear reaction was initiated - the proton-proton chain (PP chain) (Iliadis 2015). The discovery of the carbon-nitrogen-oxygen cycle (CNO cycle) in Bethe (1939), won Bethe the Nobel Prize in 1967 (Lee and Brown 2007). Bethe (1939) discuss the ${}^2_1\mathrm{H} + {}^2_1\mathrm{H}$ and ${}^4_2\mathrm{He} + {}^4_2\mathrm{He}$ reactions, but not the ${}^3_1\mathrm{H} + {}^3_1\mathrm{H}$ reaction[1], today known as the PP3 branch.

In this paper, we will model the three PP branches PP1, PP2, and PP3, and the CNO cycle. We will estimate the neutrino energies from the reactions, and the temperature intervals where the cycle and branches dominates. Our findings will be compared to previous work (e.g. Adelberger *et al.* 2011, Gudiksen 2022, The Borexino Collaboration 2018), to determine the quality of the model. The nuclear reactions are presented in Section II, together with the model parameters. All the results are found in Section III, and will be discussed in Section IV. Our conclusion is reached in Section V.

II. METHOD

A. Nuclear reactions

When hydrogen fuses into helium, 26.732 mega electron volts (MeV) are released. This energy is equivalent to the mass difference between one ${}^4_2\mathrm{He}$ nucleus and four ${}^1_1\mathrm{H}$ nuclei. The reaction

$$4\,{}^1_1\mathrm{H} \rightarrow {}^4_2\mathrm{He} \tag{1}$$

happens either through the proton-proton chain (PP chain) or the carbon-nitrogen-oxygen cycle (CNO cycle) (Gudiksen 2022).

1. *The PP chain*

The PP chain consists of three branches PP1, PP2, and PP3. Common for all of the branches are the reactions where two ${}^1_1\mathrm{H}$ nuclei combine into one ${}^2_1\mathrm{D}$ nucleus, and one ${}^2_1\mathrm{D}$ and ${}^1_1\mathrm{H}$ nucleus fuse into a ${}^3_2\mathrm{He}$ nucleus[2].

$${}^1_1\mathrm{H} + {}^1_1\mathrm{H} \rightarrow {}^2_1\mathrm{D} + e^+ + \nu_e + 0.155\,\mathrm{MeV} \tag{2}$$

$${}^2_1\mathrm{D} + {}^1_1\mathrm{H} \rightarrow {}^3_2\mathrm{He} + 5.494\,\mathrm{MeV} \tag{3}$$

In the first reaction, one positron is created in order to conserve the charge. This will quickly annihilate with an electron and release two photons γ, each of energy 0.511 MeV. Since this energy is absorbed in the stellar core, the energy output for this reaction is

$$Q'_{pp} = (0.155 + 2 \cdot 0.511)\,\mathrm{MeV} = 1.177\,\mathrm{MeV}, \tag{4}$$

where *pp* indicates the two protons in the hydrogen cores. In addition to the positron, an electron-related neutrino (neutrino, hereafter) is created, carrying 0.265 MeV of energy. This energy is lost and does not contribute to the energy output.

* https://github.com/JohanCarlsen/

[1] When asked about why he had not considered this reaction, Bethe answered: "I didn't think of it!" (Lee and Brown 2007).

[2] This "branch" is called PP0 in the scripts. This is not a branch of the PP chain, as it does not produce ${}^4_2\mathrm{He}$.

The **PP1** branch directly converts ${}^3_2$He into ${}^4_2$He.

$$ {}^3_2\mathrm{He} + {}^3_2\mathrm{He} \rightarrow {}^4_2\mathrm{He} + 2\,{}^1_1\mathrm{H} + 12.860\,\mathrm{MeV} \quad (5) $$

Note that this reaction requires two ${}^3_2$He nuclei, meaning that the previous reactions need to happen twice. We will assume that the produced deuterium is immediately consumed by the next step to produce ${}^3_2$He. This means that the reaction rate is the same for both reactions (see Section II C). For temperatures below 1 MK to 18 MK, the PP1 branch is dominant (Iliadis 2015).

In the **PP2** branch, ${}^7_4$Be and ${}^7_3$Li are created and consumed within the branch.

$$ {}^3_2\mathrm{He} + {}^4_2\mathrm{He} \rightarrow {}^7_4\mathrm{Be} + 1.586\,\mathrm{MeV} \quad (6) $$

$$ {}^7_4\mathrm{Be} + e^- \rightarrow {}^7_3\mathrm{Li} + \nu_e + 0.049\,\mathrm{MeV} \quad (7) $$

$$ {}^7_3\mathrm{Li} + {}^1_1\mathrm{H} \rightarrow 2\,{}^4_2\mathrm{He} + 17.346\,\mathrm{MeV} \quad (8) $$

In the second step, ${}^7_4$Be decays into ${}^7_3$Li. 90 % of the time, ${}^7_3$Li is produced in its ground state. Then the neutrino carries 0.86 MeV. If the ${}^7_3$Li is produced in an excited state, the neutrino carries 0.38 MeV (Gudiksen 2022) . We will consider the weighted average of 0.815 MeV. This electron capture by ${}^7_4$Be has an upper limit at temperatures below 10^6 K of $N_A\lambda_{e7} \leq 1.57 \cdot 10^{-7}/n_e$ (see Section II C), where $N_A = 6.022 \cdot 10^{23}\,\mathrm{mol}^{-1}$ is Avogrado's number. The PP2 branch is dominant for temperatures between 18 MK and 25 MK (Iliadis 2015).

Similar to the PP2 branch, the **PP3** branch creates and consumes elements. Also, the first reaction is the same as the first reaction in the PP2 branch.

$$ {}^3_2\mathrm{He} + {}^4_2\mathrm{He} \rightarrow {}^7_4\mathrm{Be} + 1.586\,\mathrm{MeV} \quad (9) $$

$$ {}^7_4\mathrm{Be} + {}^1_1\mathrm{H} \rightarrow {}^8_5\mathrm{B} + 0.137\,\mathrm{MeV} \quad (10) $$

$$ {}^8_5\mathrm{B} \rightarrow {}^8_4\mathrm{Be} + e^+ + \nu_e + 7.345\,\mathrm{MeV} \quad (11) $$

$$ {}^8_4\mathrm{Be} \rightarrow 2\,{}^4_2\mathrm{He} + 2.995\,\mathrm{MeV} \quad (12) $$

In the third step, ${}^8_5$B goes through a radioactive β-decay. Here, high-energy neutrinos are created, carrying 6.711 MeV. As stated by Iliadis (2015), the PP3 branch is dominant for temperatures above 25 MK.

The energy outputs Q', neutrino energies Q_ν, and symbols are listed in Table I. The energy output takes annihilation energy into account. For each positron created, $2 \cdot 0.511$ MeV is added to the released energy. The symbols are corresponding to the particle (i.e. p for protons, d for deuterium, and e for electrons) or the mass numbers of the elements in the reaction (e.g. 3 for helium-3, 4 for helium-4). Symbols with an apostrophe have common mass numbers in their reactions.

Nuclear reactions of the PP chain

Branch	**Q′ [MeV]**	**Q$_\nu$ [MeV]**	**Symbol**
All	1.177	0.265	pp
	5.494		pd
1	12.860		33
2 & 3	1.586		34
2	0.049	0.815	e7
	17.346		17’
3	0.137		17
	8.367	6.711	8
	2.995		8’

Table I: Energy outputs Q', neutrino energies $Q\nu$, and the reaction symbols for the PP branches. From Gudiksen (2022).

2. *The CNO cycle*

In the CNO cycle, the elements carbon, nitrogen, and oxygen are used as catalysts to produce helium. This process is only effective at temperatures above 10^7 K (Gudiksen 2022), and is the dominant producer of ${}^4_2$He at temperatures above 10^8 K (Iliadis 2015).

$$ {}^{12}_6\mathrm{C} + {}^1_1\mathrm{H} \rightarrow {}^{13}_7\mathrm{N} + 1.944\,\mathrm{MeV} \quad (13) $$

$$ {}^{13}_7\mathrm{N} \rightarrow {}^{13}_6\mathrm{C} + e^+ + \nu_e + 0.491\,\mathrm{MeV} \quad (14) $$

$$ {}^{13}_6\mathrm{C} + {}^1_1\mathrm{H} \rightarrow {}^{14}_7\mathrm{N} + 7.551\,\mathrm{MeV} \quad (15) $$

$$ {}^{14}_7\mathrm{N} + {}^1_1\mathrm{H} \rightarrow {}^{15}_8\mathrm{O} + 7.297\,\mathrm{MeV} \quad (16) $$

$$ {}^{15}_8\mathrm{O} \rightarrow {}^{15}_7\mathrm{N} + e^+ + \nu_e + 0.735\,\mathrm{MeV} \quad (17) $$

$$ {}^{15}_7\mathrm{N} + {}^1_1\mathrm{H} \rightarrow {}^{12}_6\mathrm{C} + {}^4_2\mathrm{He} + 4.966\,\mathrm{MeV} \quad (18) $$

In total, four hydrogen nuclei combine in order to make one ${}^4_2$He nucleus. Two neutrinos are created, one in step 2 (0.707 MeV) and one in step 5 (0.997 MeV). The proton capture by ${}^{14}_7$N in the fourth step is the slowest reaction, meaning that by the time this step is completed, most of the initial carbon in the core will be transformed into nitrogen (Wiescher *et al.* 2010). From this reasoning, we will only need to include the fourth reaction in the CNO cycle when calculating the energy production rate for the entire cycle. The ${}^{12}_6$C in the stellar core can be formed directly in a collision between three α-particles (Bethe 1939). In Table II, all of the energy outputs Q', neutrino energies Q_ν, and symbols are listed. As for the PP chain, annihilation energy is added to the energy outputs.

Nuclear reactions of the CNO cycle

Step	**Q′[MeV]**	**Q$_\nu$ [MeV]**	**Symbol**
1	1.944		p12
2	1.513	0.707	13
3	7.551		p13
4	7.297		p14
5	1.757	0.997	15
6	4.966		p15

Table II: Energy outputs Q', neutrino energies Q_ν, and the reaction symbol for the CNO cycle. From Gudiksen (2022).

B. Number density

For an element k, the number density is given by

$$n_k = \frac{\rho f_k}{A m_u}, \tag{19}$$

where ρ is the core mass density, f_k is the fractional abundance by weight of element k, A is the atomic number, and $m_u = 1.661 \cdot 10^{-27}\, kg$ is the atomic mass unit. In Table III, the mass fractions of some of the elements present in the stellar cores are listed. We assume that the fractions are independent of radius and that they are the same for each of the cores we model.

Element	Mass fraction (f_k)
$^{1}_{1}$H	0.7
$^{3}_{2}$He	10^{-10}
$^{4}_{2}$He	0.29
$^{7}_{3}$Li	10^{-7}
$^{7}_{4}$Be	10^{-7}
$^{14}_{7}$N	10^{-11}

Table III: Fractional weight abundance of some of the elements in the stellar cores.

C. Reaction rate

The number of reactions between element i and k per unit mass per second is given by

$$r_{ik} = \frac{n_i n_k}{\rho(1+\delta_{ik})}\lambda_{ik}\,, \tag{20}$$

where n_j is the number density of element j, ρ is the core mass density of the star, and δ_{ik} is the Kronecker delta function. The proportionality function λ_{ik} denotes the reaction rates as a function of temperature, in units of $\mathrm{m^3 s^{-1}}$.

D. Energy output

When two elements fuse together to make a heavier element, the released energy is calculated from the mass difference as

$$\delta E = -\delta m c^2, \tag{21}$$

where δm is the change in mass from before to after the reaction, and $c = 2.998 \cdot 10^8$ $\mathrm{ms^{-1}}$ is the speed of light in vacuum.

E. Energy production

For a given reaction, the energy production is given by

$$\epsilon = \sum Q'_{ik} r_{ik}, \tag{22}$$

where Q'_{ik} is the energy output including annihilation energy, and r_{ik} is the reaction rate for that reaction.

When we simulate the energy production in the stellar core, we have to make sure that a reaction does not consume more of an element than the previous step has produced. As an example, the PP1 branch requires two $^{3}_{2}$He nuclei, meaning that the reaction rate for PP1 has to be limited. We solve this by summing over the reaction rates for all the reactions that require an element and dividing the reaction rate for where the element is produced by this sum. For PP1, the energy produced becomes

$$R_{\mathrm{PP1}} = \frac{r_{\mathrm{PP0}}}{2 \cdot r_{\mathrm{PP1}} + r_{\mathrm{PP2}}} \tag{23}$$

$$\epsilon_{\mathrm{PP1}} = \epsilon_{\mathrm{PP1}} \cdot R \tag{24}$$

where we have taken into consideration that $^{3}_{2}$He is required both in the PP1 branch (twice) and in the first step of PP2 or PP3. R_{PP1} is a limitation factor, and the r's are reaction rates for the branches involved. This method is analogous to every reaction that produces an element that is required by one or several others.

When calculating the total energy production for the PP branches, we have to consider that not all of the energy produced in the common first step contributes to the energy production from the individual branches. This is solved as follows.

$$\epsilon^1_{\mathrm{PP1}} = \epsilon_{\mathrm{PP0}} \cdot \frac{r_{33}}{2 r_{pp}} \tag{25}$$

$$\epsilon^1_{\mathrm{PP2\&3}} = \epsilon_{\mathrm{PP0}} \cdot \frac{r_{34}}{r_{pp}} \tag{26}$$

where superscript 1 denotes the first reaction of the branch. In this way, only the energy from the PP0 "branch" that goes into each of the subsequent branches is added.

F. The Gamow peak

In Eq. 20, the λ_{ik} factor is a complex function. Written out, it looks like

$$\lambda_{ik} = \sqrt{\frac{8}{m\pi(k_B T)^3}} \int_0^\infty \exp\left\{-\frac{E}{k_B T}\right\} E\sigma(E)\, dE, \tag{27}$$

where $m = m_i m_k/(m_i + m_k)$ is the reduced mass and E is the kinetic energy in the center of the mass system. The tunneling effect has a cross-section $\sigma(E)$, on the form

$$\sigma(E) = E^{-1} S(E) \exp\left\{-\sqrt{\frac{m}{2E}}\frac{Z_i Z_k e^2 \pi}{\epsilon_0 h}\right\}, \tag{28}$$

where $S(E)$ is a slowly varying function of E, Z_i and Z_k are the atomic numbers of elements i and k, e is the elementary charge, and $h = 6.626 \cdot 10^{-}34$ $\mathrm{m^2 kgs^{-1}}$ is

Planck's constant. When taking the product of the two exponentials in Eqs. 27 and 28, the result is a curve that has its maximum at the Gamow peak. The peak is the relation between the probability of fusing elements and the speed of the nuclei in a gas. The peak represents the highest probability of fusing (Lebreton *et al.* 2014).

G. Sanity check

To check that our numerical implementations are correct, we compare them to known values for the Sun. We use $\rho_\odot = 1.62 \cdot 10^5$ kgm^{-3} as the core mass density, and $T_\odot = 1.57 \cdot 10^7$ K as the core temperature. We also check for $T = 10^8$ K, with solar core mass density. The known values are listed in Table IV. The produced energies have been multiplied with the solar core mass density $\rho_\odot$.

Energy production in the Sun at different core temperatures

Reaction rate	Energy [Jm^{-3}s^{-1}]	
	$\mathbf{T = T_\odot}$	$\mathbf{T = 10^8}$ **K**
$r_{pp}(Q'_{pp} + Q'_{pd})\rho_\odot$	$4.04 \cdot 10^2$	$7.34 \cdot 10^4$
$r_{33}Q'_{33}\rho_\odot$	$8.68 \cdot 10^{-9}$	$1.09 \cdot 10^0$
$r_{34}Q'_{34}\rho_\odot$	$4.86 \cdot 10^{-5}$	$1.74 \cdot 10^4$
$r_{e7}Q'_{e7}\rho_\odot$	$1.49 \cdot 10^{-6}$	$1.22 \cdot 10^{-3}$
$r_{17'}Q'_{17'}\rho_\odot$	$5.29 \cdot 10^{-4}$	$4.35 \cdot 10^{-1}$
$r_{17}(Q'_{17} + Q'_{\text{decay}})\rho_\odot$	$1.63 \cdot 10^{-6}$	$1.26 \cdot 10^5$
$r_{p14}Q'_{\text{CNO}}\rho_\odot$	$9.18 \cdot 10^{-8}$	$3.45 \cdot 10^4$

Table IV: Energy production ϵ for the reactions in the PP branches and the CNO cycle in the solar core at $T = T_\odot$ and $T = 10^8$ K. Note that ϵ has been multiplied with the solar core mass density $\rho_\odot$.

III. RESULTS

A. Sanity check

We use Eq. 22 to calculate the energy production rates and compare the results to the values in Table IV. The results and relative errors are presented in Table V.

B. Neutrino energy

As stated in Section II A, the neutrino energy escapes the star. By adding together all of the Q' that goes into each branch, we can estimate how much of the energy output is lost to neutrinos. In Table VI, the mass difference energy is calculated with Eq. 21 and is the same for every PP branch and the CNO cycle. The difference between δE and Q' corresponds to the neutrino energy.

Numerical calculations of energy productions compared to the known values in Table IV

Branch	Energy [Jm^{-3}s^{-1}]			
	$\mathbf{T = T_\odot}$		$\mathbf{T = 10^8}$ **K**	
	Computed	Rel. error	Computed	Rel. error
PP0	$4.048 \cdot 10^2$	$1.980 \cdot 10^{-3}$	$7.342 \cdot 10^4$	$2.725 \cdot 10^{-4}$
PP1	$8.686 \cdot 10^{-9}$	$6.912 \cdot 10^{-4}$	$1.098 \cdot 10^0$	$7.339 \cdot 10^{-3}$
PP2	$4.866 \cdot 10^{-5}$	$1.235 \cdot 10^{-3}$	$1.745 \cdot 10^4$	$2.874 \cdot 10^{-3}$
	$5.297 \cdot 10^{-4}$	$1.323 \cdot 10^{-3}$	$4.353 \cdot 10^{-1}$	$6.897 \cdot 10^{-4}$
PP3	$1.639 \cdot 10^{-6}$	$5.521 \cdot 10^{-3}$	$1.266 \cdot 10^5$	$4.762 \cdot 10^{-3}$
CNO	$9.185 \cdot 10^{-8}$	$5.447 \cdot 10^{-4}$	$3.455 \cdot 10^4$	$1.449 \cdot 10^{-3}$

Table V: The results from our numerical calculations of the energy production of the different PP branches and the CNO cycle. Comparing with the known values in Table IV yields the relative error.

Branch	δE [MeV]	$\sum$Q′ [MeV]	E_{ν_e} [MeV]	%
PP1	26.734	26.202	0.532	1.99
PP2	26.734	26.652	1.082	4.05
PP3	26.734	19.756	6.978	26.10
CNO	26.734	25.028	1.706	6.38

Table VI: Energy lost to neutrinos (E_{ν_e}) and the percentage of the total energy output it represents. The total energy output ($\sum Q'$) is the sum of all of the Q' of each of the PP branches and the CNO cycle.

C. Relative energy production

In Figure 1, we present the relative energy productions of the PP branches and the CNO cycle for temperatures in the range 10^4 K to 10^9 K. We see that the PP1 branch is dominant up to $\sim 7.0 \cdot 10^4$ K, where PP2 takes over. From temperatures between $2.5 \cdot 10^7$ K and $1.2 \cdot 10^8$ K, PP3 is dominant, before the CNO cycle dominates at higher temperatures. We recognize the limitation for the $^7_4$Be electron capture at $T = 10^6$ K. The energy productions are normalized by the sum of all of the produced energy at each temperature.

D. Gamow peaks

The Gamow peaks are presented in Figure 2. The curves are normalized by the individual peaks. We use energies in the range 10^{-17} J to 10^{-13} J. The figure shows energies in keV, and are cropped between 1 keV and 100 keV. We see that the *pp*-reaction (2) and the *pd*-reaction (3) have their energies around 6 keV, the 17'-reaction (7) and the 17-reaction (8) from 15 keV to 19 keV, and the rest between 22 keV and 28 keV. The energies at which each reaction has its Gamow peak are listed in Table VII, in ascending order. As stated by Lebreton *et al.* (2014), these energies determine the highest probability to fuse.

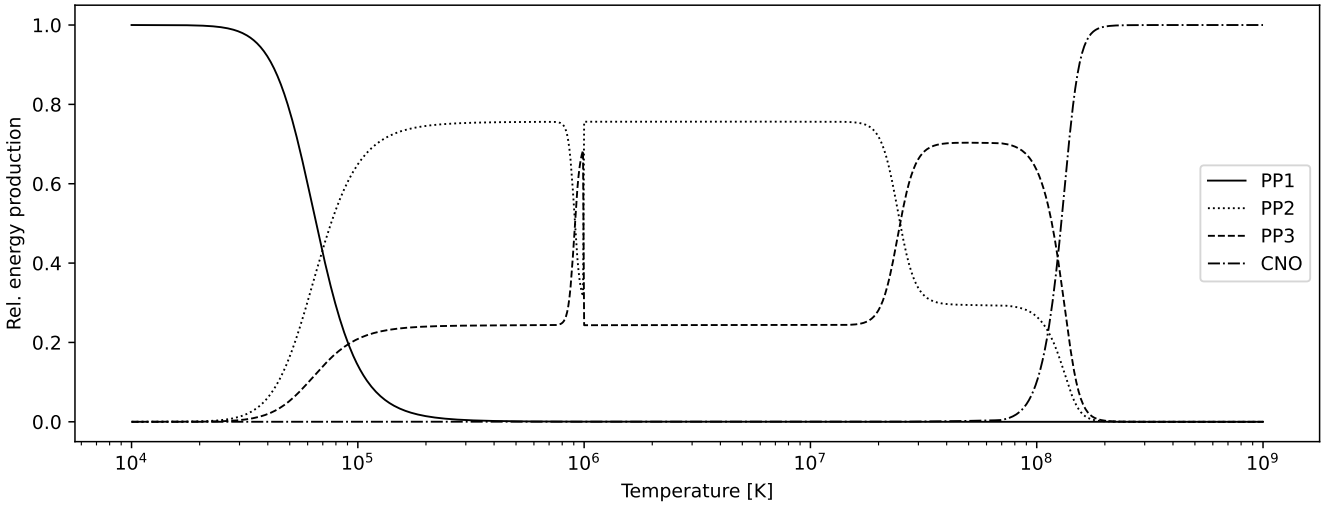

Figure 1: The relative energy production for the PP branches and the CNO cycle, for $T \in [10^4, 10^9]$ K. At each T, the energies are normalized by the sum of all processes (i.e. sum of all PP branches and the CNO cycle).

Gamow peak energies

Symbol	**E(peak) [keV]**
pp	6.071
pd	6.719
17'	15.251
17	18.505
33	22.044
34	23.083
p12 & p13	24.620
p14 & p15	27.497

Table VII: Energies in keV in ascending order for the reactions in the PP branches and the CNO cycle.

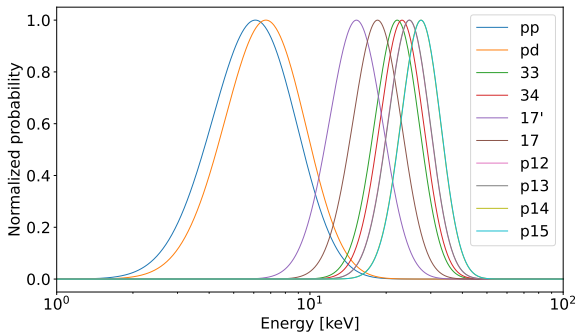

Figure 2: The curves are the product of the two exponentials in Eqs. 27 & 28. The extreme points are the Gamow peaks, which correspond to the highest probability for the elements to fuse (Lebreton *et al.* 2014).

IV. DISCUSSION

When comparing our numerically calculated energy outputs, the relative errors shown in Table V are at most of the order 10^{-3}, both for the solar core temperature and 10^8 K. This corresponds to a maximum of 0.1 % deviation from the known values.

In Table VI, our computed neutrino energies for the PP branches and the CNO cycle are in strong correlation to the values from Gudiksen (2022) in Table I. The Borexino Collaboration (2018) suggests an energy of 0.267 MeV for the neutrino in 2 and 0.862 MeV for the neutrino in 7. For the $^8_5$B decay, Gudiksen (2022) states that the neutrino energies follow a continuum and that the neutrino energy for the $^8_5$B decay in Table I is the average energy.

The reported temperature dominance domains for the PP branches and the CNO cycle in Section III C are in conflict with Iliadis (2015), regarding the PP1 and PP2 branches. In his book, Iliadis assumes a gas composition of hydrogen and helium, where the fractional abundance is 0.50 for each when presenting his temperature dominance intervals for the PP branches. For the PP3 branch and the CNO cycle, our results regarding the dominant energy producer are in agreement with both Gudiksen (2022) and Iliadis (2015).

The Gamow peaks presented in Figure 2 and energies in Table VII show that all of the reactions aside from *pp* and *pd* have their Gamow peak energy in the range 15 keV to 27.5 keV, corresponding to the solar Gamow peak (Bonetti *et al.* 1999). Our calculations are in agreement with the reported energies for the Gamow peaks in Adelberger *et al.* (2011).

V. CONCLUSION

In Section II, we present the PP chain and the CNO cycle which are the only known processes for transforming hydrogen into helium in stellar cores (Gudiksen 2022). We also describe the calculations behind the energy production, and the assumptions regarding the element abundance used in this paper. How we calculate the Gamow peak and the meaning of these values are also included in this section. In order to control that our numerical implementation is satisfactory, we add a sanity check, which allows us to compare our calculations to known values for the Sun.

All of our results are presented in Section III. We use the mass defect formula to estimate the total energy output, and from that deduce the neutrino energy for the individual processes. By computing the relative energy production, we find the temperature domains where the different processes are dominant.

From our discussion in Section IV, we find that our numerical model fits well with the data. Our estimates for the neutrino energies are 0.532 MeV for the PP1 branch, 1.082 MeV for the second, 6.978 MeV for the third branch, and 1.706 for the CNO cycle. These values are in agreement Gudiksen (2022). More precise measurements have been done by The Borexino Collaboration (2018), which suggests a slightly higher neutrino energy for the CNO cycle.

We also find that the Gamow peak energies for the PP branches and the CNO cycle are within the solar Gamow peak (Bonetti *et al.* 1999), and are in agreement with the results in Adelberger *et al.* (2011).

As mentioned in our discussion of the temperature domains, the fractional mass abundance in Iliadis (2015) differs from ours. Further research may be done with different stellar core compositions, as well as including the radius-dependency these fractions have. Furthermore, data produced during the Borexino experiment can be used as a mark in order to compose more accurate models for computing solar neutrino energies.

REFERENCES

Adelberger, E. G., A. García, R. G. H. Robertson, K. A. Snover, A. B. Balantekin, K. Heeger, *et al.* (2011), Rev. Mod. Phys. **83**, 195.

Bethe, H. A. (1939), Phys. Rev. **55**, 434.

Bonetti, R., C. Broggini, L. Campajola, P. Corvisiero, A. D'Alessandro, M. Dessalvi, *et al.* (1999), Phys. Rev. Lett. **82**, 5205.

Gudiksen, B. V. (2022), "Ast3310: Astrophysical plasma and stellar interiors," Lecture notes.

Iliadis, C. (2015), *Nuclear physics of stars* (Wiley-VCH).

Lebreton, Y., M.-J. Goupil, and J. Monralabán (2014), EAS Publications Series **65**, 99.

Lee, S., and G. E. Brown (2007), Biogr. Mems Fell. R. Soc. **53**, 1.

The Borexino Collaboration, (2018), Nature **562**, 505.

Wiescher, M., J. Görres, E. Uberseder, G. Imbriani, and M. Pignatari (2010), Annual Review of Nuclear and Particle Science **60** (1), 381.